Dalton Transactions

PAPER

View Article Online
View Journal | View Issue

Cite this: *Dalton Trans.*, 2015, **44**, 5555

Binuclear platinum–iridium complexes: synthesis, reactivity and luminescence†‡

Brian T. Sterenberg,[a,b] Christian T. Wrigley[a] and Richard J. Puddephatt*[a]

Received 23rd December 2014,
Accepted 9th February 2015

DOI: 10.1039/c4dt03966a

www.rsc.org/dalton

The chemistry of the heterobinuclear platinum–iridium complex $[PtIr(CO)_3(\mu\text{-dppm})_2][PF_6]$, **1**, dppm = $Ph_2PCH_2PPh_2$, is described. The reaction of a hydride with **1** gave $[HPtIr(CO)_2(\mu\text{-dppm})_2]$, by displacement of the carbonyl ligand from platinum, while reaction of **1** with dihydrogen, hydrogen chloride or Ph_2MeSiH gave the fluxional complex $[PtIrH_4(CO)(\mu\text{-dppm})_2][PF_6]$, $[PtIrH_2Cl_2(CO)(\mu\text{-dppm})_2][PF_6]$, or $[PtIrH(SiMePh_2)(CO)_2(\mu\text{-dppm})_2][PF_6]$, respectively, by oxidative addition at iridium. Complex **1** reacted, often regioselectively, with several alkynes to give the $\mu\text{-}\eta^1,\eta^1$ bridging alkyne complexes $[PtIr(\mu\text{-RCCR'})(CO)_2(\mu\text{-dppm})_2][PF_6]$, R = H, R' = Ph, 4-$C_6H_4Me$, CO_2Me; R = Ph, R' = CO_2Me; R = R' = CO_2Me. The complex $[PtIr(\mu\text{-HCC-4-}C_6H_4Me)(CO)_2(\mu\text{-dppm})_2][PF_6]$ reacted reversibly with CO to give $[PtIr(\mu\text{-HCC-4-}C_6H_4Me)(CO)_3(\mu\text{-dppm})_2][PF_6]$ and $[PtIr(CO)_3(\mu\text{-dppm})_2][PF_6]$, **1**. With HCl, $[PtIr(\mu\text{-HCC-4-}C_6H_4Me)(CO)_2(\mu\text{-dppm})_2][PF_6]$ reacted to give $[PtIrHCl(\mu\text{-HCC-4-}C_6H_4Me)(CO)_2(\mu\text{-dppm})_2][PF_6]$, by oxidative addition at iridium, and then the alkenylplatinum derivative $[PtIrCl\{HC{=}CH(4\text{-}C_6H_4Me)\}(CO)_2(\mu\text{-dppm})_2][PF_6]$. $[PtIr(\mu\text{-HCC-4-}C_6H_4Me)(CO)_2(\mu\text{-dppm})_2][PF_6]$ reacted slowly with dihydrogen to give 4-$MeC_6H_4CH{=}CH_2$ and $[PtIrH_4(CO)(\mu\text{-dppm})_2][PF_6]$. The complex $[PtIr(\mu\text{-HCCPh})(CO)_2(\mu\text{-dppm})_2][PF_6]$ is intensely luminescent in solution at room temperature, with features characteristic of a d^8–d^8 face-to-face complex.

Introduction

The study of heterobimetallic or cluster complexes has relevance in the testing of current bonding concepts,[1,2] in modelling the reactions proposed to occur during catalysis using bimetallic catalysts[3,4] and, in some cases, in developing photonic devices.[5] The concepts that are implicit in Wade's rules and explicit in the isolobal analogy have been crucially important in providing a framework for understanding complex chemistry and in predicting future developments.[1,2] Bimetallic Pt–Ir, Pt–Re and Pt–Sn catalysts are universally used in reforming petroleum, to increase the octane number by converting linear alkanes to branched or cyclic alkanes, alkenes and aromatics, and they can also be used for catalytic oxidation in fuel cells and for liquid phase catalytic isotope exchange.[3,4] The ability of a second metal complex to interact with a square planar d^8 metal centre, such as a platinum(II) centre, is proving to be important in the development of brightly phosphorescent complexes.[5]

In this context, we and others have been interested in the synthesis of heterobinuclear complexes with platinum–metal bonds and in studies of their reactivity and photophysical properties.[3,5,6–11] In particular, during the synthesis of $PtIr_2$ cluster complexes, two binuclear complexes containing Pt–Ir bonds bridged by bis(diphenylphosphino)methane (dppm) ligands were prepared as shown in Scheme 1. In the cationic complex $[PtIr(CO)_3(\mu\text{-dppm})_2]^+$, **1**, which was isolated as the hexafluorophosphate salt, the Pt–Ir distance is 2.7674(4) Å, and the square planar platinum and trigonal bipyramidal iridium centres have 16 and 18-electron configurations respectively.[6] This article reports a study of the chemistry of complex **1**.

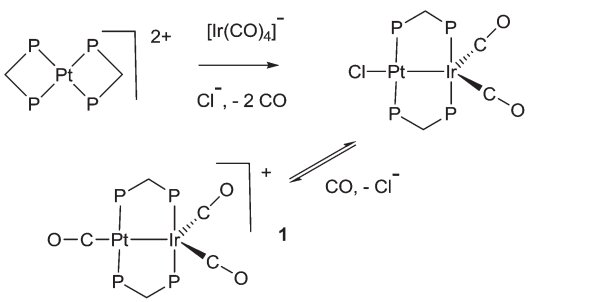

Scheme 1 Synthesis of $[PtIr(CO)_3(\mu\text{-dppm})_2][PF_6]$, **1** (P = PPh_2).

[a]*Department of Chemistry, University of Western Ontario, London, Ontario, Canada N6A 5B7. E-mail: pudd@uwo.ca*
[b]*Department of Chemistry and Biochemistry, University of Regina, Regina, Saskatchewan, Canada*

†This article is dedicated to the memory of Professor Ken Wade, whose work has been so important in understanding not only the structure but also the reactivity of complexes with metal–metal bonds.

‡CCDC 1040456–1040458 for **6a–6c**. For crystallographic data in CIF or other electronic format see DOI: 10.1039/c4dt03966a

Results and discussion

Hydride complexes derived from complex 1

Some hydrido derivatives derived from complex **1** are shown in Scheme 2. We were not able to grow crystals of any of the hydrides suitable for structure determination, but the main features of the complexes could be determined spectroscopically.

Complex **2** was most readily prepared by reaction of complex **1** with sodium triethylborohydride. It is characterized by a hydride resonance at δ −3.3 with a coupling constant ^1J(PtH) of 1123 Hz, showing that the hydride is bound as a terminal ligand to platinum. Homobinuclear complexes $[HPtPt(L)(\mu\text{-dppm})_2]^+$, with the hydride *trans* to a Pt–Pt bond, give somewhat smaller values of ^1J(PtH), such as ^1J(PtH) 990 Hz when L = CO, but this increases to 1326 Hz in $[HPtPt(CO)_2(\mu\text{-dppm})_2]^+$, which is isoelectronic to complex **1**.[12] The CH_2 protons of the dppm ligands in **2** appeared as a single multiplet, showing that there is an effective plane of symmetry containing the $PtIrP_4C_2$ atoms of the $PtIr(\mu\text{-dppm})_2$ unit.[8,9,12–14] The ^{31}P NMR spectrum contained two dppm resonances at δ 16.1, ^1J(PtP) 2873 Hz, and −16.4, ^2J(PtP) 69 Hz, for the PtP and IrP groups respectively.

The reaction of complex **1** with dihydrogen gave the product of double oxidative addition $[PtIrH_4(CO)(\mu\text{-dppm})_2][PF_6]$, **3** (Scheme 2). Complex **3** was also formed during attempted synthesis of **2** by the reaction of **1** with $Na[BH_4]$ using an aqueous workup procedure, and this reaction was later shown to involve reaction of **2** with dihydrogen in the presence of a proton source (Scheme 2). The presence of four hydride ligands in complex **3** was readily shown by the ^{1}H NMR spectrum, which contained four equal intensity resonances in the hydride region (Fig. 1). At room temperature, the spectrum contained two well resolved hydride resonances and two very broad ones, which sharpened on cooling to −30 °C (Fig. 1). There were two resonances for the CH_2P_2 protons of the dppm ligands, which were broad at room temperature but which also sharpened at −30 °C. These data suggest that complex **3** is fluxional in such a way that two of the hydride ligands and the $CH^xH^yP_2$ protons can become equivalent at higher temperatures, while two of the hydrides do not exchange. The activation energies estimated using the Eyring equation from coalescence of the $CH^xH^yP_2$ protons [coalescence temperature, T_c = 323 K, $\Delta\nu$ = 405 Hz] and the hydride H^c,H^d protons [coalescence temperature, T_c = 333 K, $\Delta\nu$ = 750 Hz] were 61.1 and 61.3 kJ mol^{-1} respectively in $C_2D_2Cl_4$ solution. These values are equal within experimental error [61(1) kJ mol^{-1}] and indicate that a common step is rate determining. The two hydrides which do not exchange are identified as a terminal PtH group [δ −3.90, ^1J(PtH) 1225 Hz, H^a] and a terminal IrH group [δ −8.17, no PtH coupling resolved, H^b], while the two that do exchange are identified as a bridging hydride [δ −9.52, ^1J(PtH) 540 Hz, H^c] and a terminal IrH group [δ −12.02, ^3J(PtH) *ca.* 90 Hz, H^d]. There are four potential isomers of complex **3** labelled as **3a–3d** in Scheme 3, of which **3a**, **3b** and **3d** contain a single bridging hydride ligand and **3c** contains two bridging hydride ligands. The ground state structure is likely to be **3a** or **3b**, in each of which the bridging hydride is *trans* to a terminal hydride ligand on iridium, and so more nucleophilic than the hydride *trans* to carbonyl on iridium. In order to give the observed spectra, the slow step in the fluxionality should exchange positions of H^c and H^d and also generate a mirror plane containing the $PtIrP_4C_2$ atoms of the $PtIr(\mu\text{-dppm})_2$ unit. We suggest that the motion involves mostly rotation of the $IrH_3(CO)$ unit about the PIrP axis, in a windscreen wiper fashion (Scheme 3). From **3a**, only anticlockwise rotation is possible because the carbonyl group cannot pass through the Pt–Ir bond. Conversion of **3a** to **3b** involves inversion of H^c through the Pt–Ir bond, **3b** to **3c** involves H^b also moving into a bridging position, and **3c** to **3d** involves moving H^c out of the bridging position (**3c** could be a transition state rather than an intermediate, but the transition

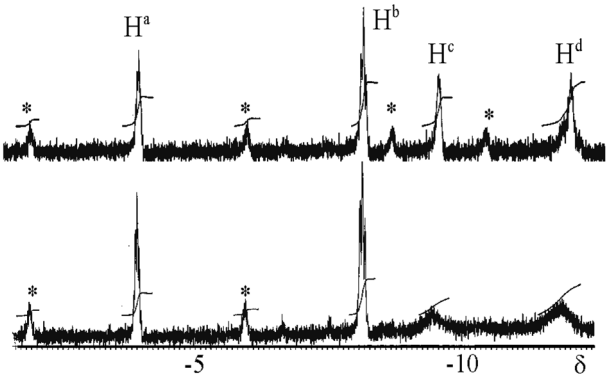

Fig. 1 ^{1}H NMR spectra (300 MHz) of complex **3**: above at −30 °C; below at 20 °C. The asterisks * indicate ^{195}Pt satellite spectra.

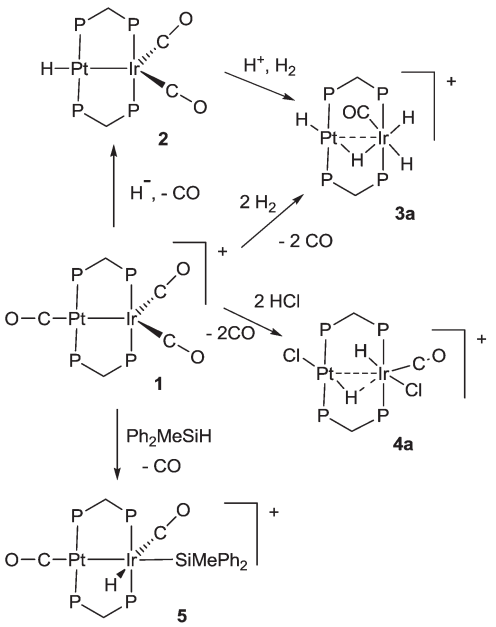

Scheme 2 Synthesis and possible structures of hydride derivatives **2–5** (P = PPh_2).

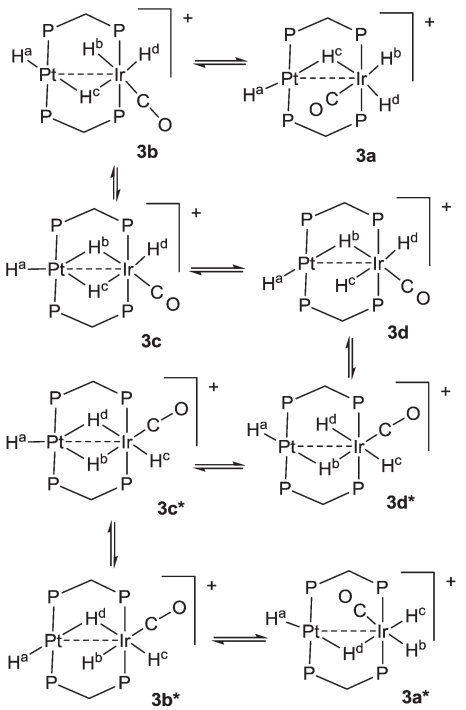

Scheme 3 Proposed fluxionality of complex **3**.

state is likely to have a roughly linear PtHIr group). This completes the first half of the motion, and is followed by inversion of H^b in **3d** through the Pt–Ir bond to give **3d*** and then further anticlockwise rotation gives in turn **3c***, **3b*** and **3a***. No further anticlockwise rotation is possible, and clockwise rotation from **3a*** simply reverses the sequence. It is the **3d** to **3d*** step which leads to effective equivalence of the H^c and H^d hydrides and creates the effective mirror plane needed to give equivalence of the $CH^xH^yP_2$ protons. The hydride H^a remains bonded to platinum and H^b remains on iridium in the position *trans* to CO throughout the rotation and, although it is possible to envisage ways in which exchange with H^c or H^d might occur,[12,14] it is evident that any such exchange must have a significantly higher activation energy.

The reaction of complex **1** with excess HCl gave the complex $[PtIrH_2Cl_2(CO)(\mu\text{-dppm})_2][PF_6]$, **4**, with loss of CO (Scheme 2).

Complex **1** also reacted with one equivalent of HCl but a mixture of products was obtained which could not be characterized. Complex **4** gave two hydride resonances in the ^1H NMR spectrum at δ −15.0 [t, ^2J(PH) = 10 Hz, no resolved coupling to platinum] and −15.5 [s, ^1J(PtH) = 858 Hz] which can be assigned to IrH and PtH groups, respectively. There were two resonances for the $CH^xH^yP_2$ protons of the dppm ligands, indicating the absence of a mirror plane containing the $PtIrP_4C_2$ atoms. The ^{13}CO NMR spectrum contained a single resonance with a coupling constant ^2J(PtC) of 180 Hz, which is too small for a direct Pt–CO bond, indicating that the carbonyl group is bound to iridium.[6,7] The ^{31}P NMR spectrum contained three resonances, which were readily assigned to the PtP groups [δ −7.8, ^1J(PtP) 2344 Hz], the IrP groups [δ −6.3] and the $[PF_6]^-$ anions [δ −143.3, ^1J(PF) 711 Hz]. There was no evidence of fluxionality of complex **4**. Several isomers of **4** are possible but only one was observed and the structure **4a** (Scheme 2) is considered most consistent with the NMR data. At the platinum centre, the coupling constant ^1J(PtH) = 858 Hz is lower than expected for a simple terminal hydride and higher than for a symmetrical bridging hydride, but it is consistent with an unsymmetrical bridging hydride or a hydride bound to a 5-coordinate platinum(II) centre.[14,15] For example, the T-frame Pt–Pt bonded complex $[HClPt(\mu\text{-dppm})_2PtH]^+$ gives ^1J(PtH) = 1360 and 962 Hz for the 4- and 5-coordinate platinum(II) centres respectively, with a long range coupling constant ^2J(PtH) = 212 Hz for the hydride at the 4-coordinate centre *trans* to the Pt–Pt bond.[14] At the iridium centre of **4**, the hydride shows no resolved long range coupling to platinum while the carbonyl does, suggesting that the carbonyl group is *trans* to the Pt···Ir bond.

The reactions of **1** to give **3** or **4** occur by double oxidative addition of H_2 or HCl respectively, and may be considered to convert Pt(I)Ir(0) in **1** to Pt(II)Ir(III) in **3** or **4**. In each case, there must be an intermediate formed by a single oxidative addition step, but it has not been possible to characterize it. We therefore studied reactions of complex **1** with silane derivatives, hoping that, after the first oxidative addition, the bulky silyl group might prevent a second addition. The reagents Ph_3SiH or $(PhCH_2)_3SiH$ failed to react with **1**, while Ph_2SiH_2 and $PhSiH_3$ reacted but gave products which could not be characterized. However, excess Ph_2MeSiH did react with complex **1** to give $[PtIrH(SiMePh_2)(CO)_2(\mu\text{-dppm})_2][PF_6]$, **5**, Scheme 2. The reaction was reversible and **5** reacted with excess CO to regenerate complex **1**. In the ^1H NMR spectrum of complex **5**, a single hydride resonance was observed at δ −8.29, with coupling constant ^2J(PtH) = 33 Hz, showing that the hydride is bound to iridium and *cis* to the Pt–Ir bond. The $^{13}C\{^1H\}$ NMR spectrum of a ^{13}CO enriched sample contained two carbonyl resonances, a triplet at δ = 186.8, ^2J(PC) = 10 Hz, with no resolved coupling to platinum, and a broad singlet at δ = 170.1, ^1J(PtC) = 1130 Hz, which are therefore assigned as IrCO and PtCO groups respectively. Important structural information is obtained from a ^{13}C (^1H coupled) NMR experiment, in which the IrCO resonance shows additional doublet splitting due to the coupling ^2J(HC) = 32 Hz. The magnitude of the ^2J(HC) coupling in **5** can be compared with the values of 43 Hz and 5 Hz found in the isomers of $[IrHBr(CO)\{Si(OEt)_3\}(dppe)]$, in which the hydride and carbonyl ligands are mutually *trans* or *cis* respectively, indicating that the *trans*-IrH(CO) group is present in **5**.[16] These data define the stereochemistry of **5** unambiguously. An unusual feature in the ^{31}P NMR spectrum of **5** is that the phosphorus atoms of the dppm ligands are all inequivalent. The PtP resonances were well separated and occurred as an "AB" multiplet at δ = −3.6 and −6.2, with ^2J(PP) = 350 Hz typical of *trans* P–Pt–P groups,[12,14,17] and with ^1J(PtP) = 2946 Hz and 3032 Hz respectively. The Ir–P resonances overlapped at δ = −20.8 in CD_2Cl_2 solution, but were resolved in CD_3CN solution. The inequivalence of the phosphorus centres is no doubt due to the bulky $SiMePh_2$ group

being locked into an unsymmetrical conformation. Complex **5** is formed by *cis* oxidative addition of the Si–H bond at the iridium centre of complex **1**, and so is a likely model for the first step in the oxidative addition of dihydrogen to **1**. The iridium centre in **1** has an 18-electron configuration so the oxidative addition should be preceded by an effective dissociative step at iridium, which might be loss of CO, heterolytic cleavage of the Pt–Ir bond or migration of a CO ligand from iridium to platinum, but loss of CO must occur at some stage during the reaction.[14] The oxidative addition of the Si–H bond to complex **1** may also provide a model for the first step in more complex reactions of silanes with dppm bridged complexes of rhodium and iridium.[18]

Reactions of alkynes with complex 1

Some reactions of complex **1** with alkynes are shown in Scheme 4. The products were characterized spectroscopically and, in three cases, by structure determination. During each reaction, one carbonyl ligand is displaced and the alkyne coordinates in the μ_2–η^1–η^1 bonding mode, which is common in dppm bridged complexes.[19] The alkynes RCCH (R = Ph, 4-C_6H_4Me, CO_2Me) react selectively to give **6a–6c** (Scheme 4), in which the CH and CR groups are bound to platinum and iridium, respectively. The symmetrical alkyne RCCR (R = CO_2Me) gave only complex **7**, but the unsymmetrical alkyne $PhCCCO_2Me$ gave an equal mixture of the two possible isomers **8a** and **8b** (Scheme 4). Diphenyl acetylene failed to react with complex **1**. No rearrangement of the complexes **6** to give the μ_2–η^2–η^2 bonded isomers, alkynyl-hydride complexes containing PtIrH(CCR) groups, or bridging vinylidene complexes containing PtIr(μ-C=CHR) groups, was observed though related reactions are known in palladium, rhodium and iridium complexes with bridging dppm ligands.[20]

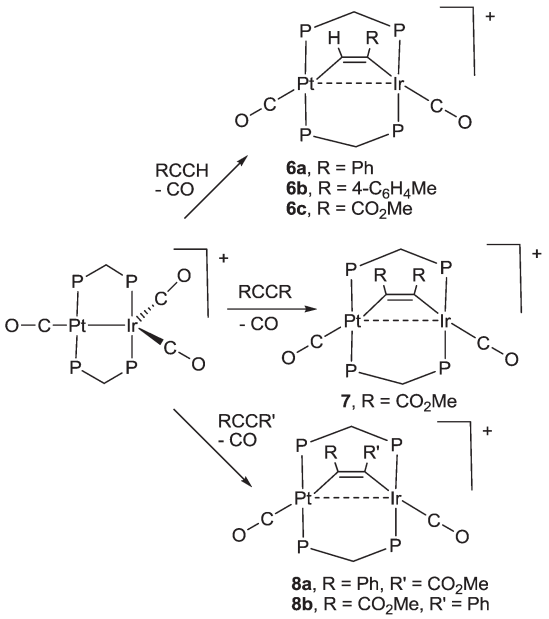

Scheme 4 Synthesis of alkyne complexes **6–8**.

The structures of complexes **6a**, **6b** and **6c** are similar and are shown in Fig. 2–4. In each case, the cation contains the expected *trans*,*trans*-PtIr(μ-dppm)$_2$ group, with a bridging alkyne and a terminal carbonyl group on each square planar metal centre. The Pt···Ir distance of 2.9180(4) Å for **6b** is longer than the sum of the covalent radii (*ca.* 2.75 Å) but shorter than the sum of the van der Waals radii (*ca.* 3.77 Å) of platinum and iridium.[21] In addition, the Pt···Ir distance for **6b** is somewhat shorter than the non-bonding distances P(1)P(4) and P(2)P(3) of 3.041(2) and 3.053(2) Å, and the angles C(4)–C(3)–Pt = 111.4(6) and C(3)–C(4)–Ir = 113.9(6)° are less than the natural sp^2 bond angle of 120°. The parameters can be compared with those for [Pt_2Cl_2(μ-PhCCH)(μ-dppm)$_2$] in which the Pt···Pt distance of 3.480(4) Å is longer and the angles C=C–Pt of 121(1) and 124(1)° are greater than 120°, indicative of no metal–metal bonding.[19] Thus, the data for **6b** indicate that there is a weak bonding interaction between the platinum and iridium atoms, which could be of the donor–acceptor or secondary metallophilic bonding type.[5–7] It should be noted that the platinum and iridium atoms could not be distinguished in the structure determination, and the assignments in Fig. 2–4 are based on the structure determination by NMR analysis described below. For example, the ^{31}P NMR spectrum of complex **6a** contained dppm resonances at δ 16.5 (IrP) and at δ 3.8 (^1J(PtP) = 3260 Hz, PtP). The ^{1}H NMR spectrum contained two resonances for the dppm methylene groups at δ 3.79 and 4.31, as expected for an A-frame structure,[22] and a resonance for the HC=C proton of the bridging alkyne at δ 7.04 [tt, ^3J(PH) 14 Hz, ^3J(PH) 1 Hz], with no resolved coupling to platinum. The ^{13}C–^{1}H HSQC NMR spectrum was used to identify the H*C* = carbon resonance at δ 119.2 [^1J(PtC) 820 Hz] and the magnitude of the ^{195}Pt^{13}C coupling constant clearly shows that this carbon atom is directly bonded to platinum. The ^{13}C–^{1}H HMBC NMR spectrum was used to identify the HC=*C*Ph carbon resonance at δ 129.9 [t, ^2J(PC) 25 Hz]. The carbonyl resonances appeared at δ 177 [t, ^2J(PC) = 10 Hz, Ir*C*O] and 184 [t, ^2J(PC) = 8 Hz, ^1J(PtC) = 1105 Hz, Pt*C*O] and a corre-

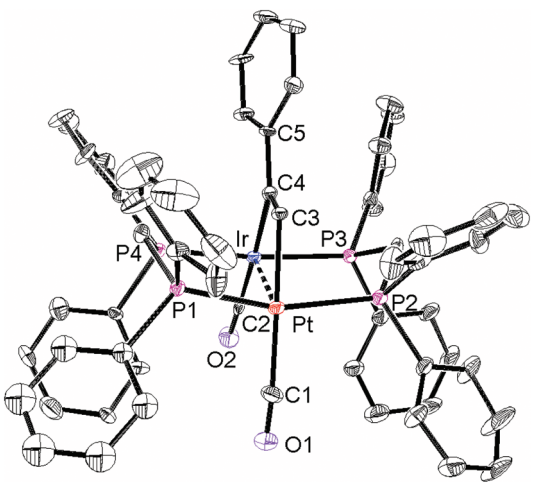

Fig. 2 The structure of the cationic complex **6a**.

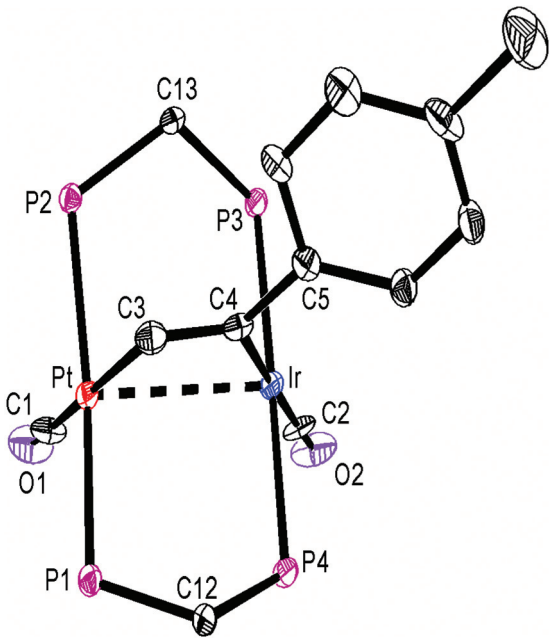

Fig. 3 The structure of the cationic complex **6b**, with phenyl groups omitted for clarity.

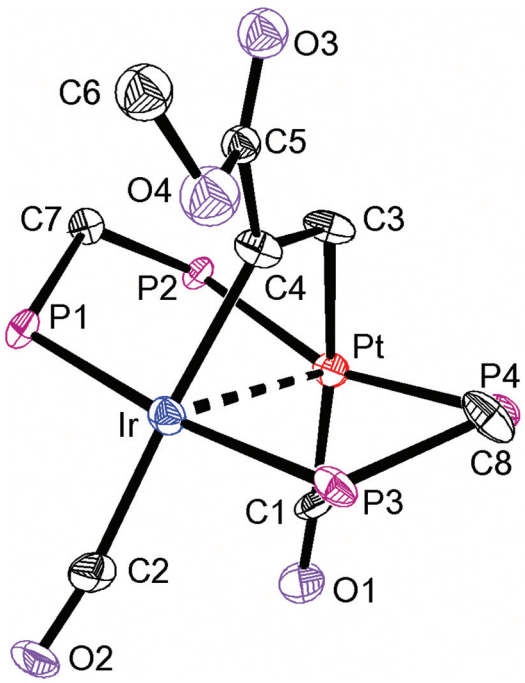

Fig. 4 The structure of the cationic complex **6c**, with phenyl groups omitted for clarity.

lation between the Pt*C*O and *H*C≡C resonances was also seen in the ^{13}C–^{1}H HMBC NMR spectra. The infrared spectrum of **6a** shows two terminal carbonyl bands at 2067 and 1964 cm^{-1}, as well as the C≡C stretch of the bridging alkyne at 1606 cm^{-1}. Thus, the structure determination by a combination of X-ray and NMR techniques leaves no doubt that the assigned structure (Scheme 4, Fig. 2) is correct. The structure obtained for complex **6a** was of low quality, and only the connectivity is established with confidence.

Table 1 Selected bond parameters (Å,°) in complexes **6b** and **6c**

	6b	6c
Pt–Ir	2.9180(4)	3.0047(4)
Pt–C(1)	1.918(9)	1.95(1)
Pt–C(3)	2.075(8)	2.069(7)
Ir–C(2)	1.96(2)	1.89(1)
Ir–C(4)	2.109(8)	2.088(8)
Pt–P(1)	2.323(2)	2.352(7)
Pt–P(2)	2.327(2)	2.292(9)
Ir–P(3)	2.298(2)	2.315(8)
Ir–P(4)	2.299(2)	2.278(9)
P(1)–Pt–P(2)	156.71(7)	161.07(8)
P(3)–Ir–P(4)	174.58(8)	173.03(8)
C(4)–C(3)–Pt	111.4(6)	108.8(6)
C(3)–C(4)–Ir	113.9(6)	118.5(6)

A comparison of some bond parameters for **6b** and **6c** is given in Table 1. One feature is that the P–Pt–P angles are more distorted from linearity (19–23°) than the P–IrP angles (5–7°). This is consistent with a donor–acceptor metal–metal interaction with iridium as the donor. In all cases, the methylene linkages of the dppm groups are folded toward the coordinated alkyne in order to minimize steric interactions between the axial phenyl rings of the dppm ligands and the alkyne.[8,12,14]

The reactivity of selected alkyne complexes has been studied. Complexes **6a** and **6b** reacted reversibly with CO to form the adducts **9a** and **9b** (Scheme 5), but **6c**, **7** and **8** did not react. The complexes **9** could not be isolated because the reactions were reversed to give **6** on evaporation of the solvents. They were characterized by reaction of **6a** or **6b** with ^{13}CO in an NMR tube. For example, the reaction of **6b** with excess ^{13}CO in CD_2Cl_2 solution at low temperature gave **9b** essentially quantitatively, with a change in colour from pink/orange to yellow. At −30 °C, two dppm resonances were observed in the ^{31}P NMR spectrum at $\delta(^{31}P)$ = 5.78 [^{1}J(PtP) = 3164 Hz, PtP] and −4.42 [IrP], with the iridium–phosphorus shifted from $\delta(^{31}P)$ = 16.19 [IrP] in **6b**. In the ^{13}C NMR spec-

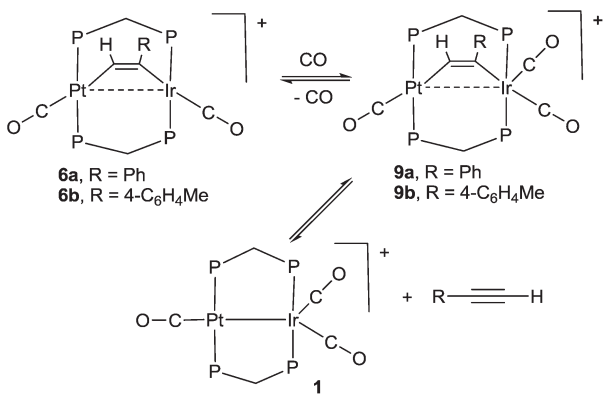

Scheme 5 Reactions of **6a** and **6b** with CO.

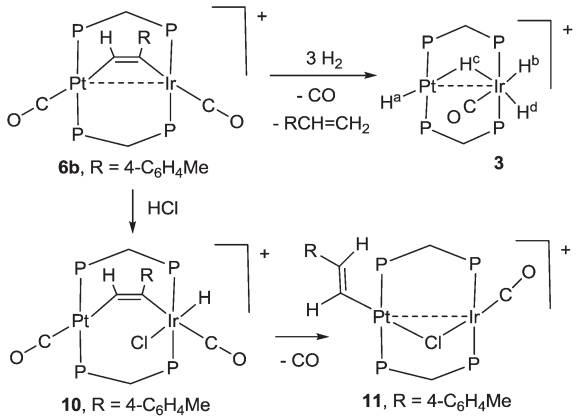

Scheme 6 Reactions of **6b** with H_2 and HCl.

trum, three carbonyl resonances were observed at $\delta(^{13}C)$ = 175.67 [m, IrCO], 178.35 [m, IrCO] and 184.80 [s, ^1J(PtC) = 1184 Hz, PtCO]. At room temperature, the IrP resonance was broad in the ^{31}P NMR spectrum and a single broad IrCO resonance was observed in the ^{13}C NMR spectrum, while resonances for **1** and 4-MeC_6H_4CCH were also observed. These data are interpreted in terms of rapid exchange between **6a** and **9a** at room temperature and with slower, partial displacement of the alkyne to give complex **1**. No CO insertion into the Ir–C or Pt–C bond of the coordinated alkyne was observed.

The reactions of complex **6b** with dihydrogen and with hydrogen chloride are shown in Scheme 6. With dihydrogen a slow reaction occurred to give the same hydride complex $[PtIrH_4(CO)(\mu\text{-dppm})_2][PF_6]$, **3**, which had previously been isolated by reaction of dihydrogen with complex **1** (Scheme 2). The alkyne group was hydrogenated to 4-methylstyrene, which was characterized by comparison of its ^1H NMR spectrum with that of an authentic sample. The reaction must involve several steps, but no intermediates were detected in significant concentration. It is therefore likely that an initial oxidative addition of dihydrogen, probably to the iridium centre, is the slow step in the sequence. The hydrogenation of phenylacetylene to styrene has been observed previously with the homobinuclear complexes $[Ir_2(\mu\text{-S})(CO)_2(\mu\text{-dppm})_2]$ and $[Rh_2Cl_2(\mu\text{-CO})(\mu\text{-dppm})_2]$, but the alkyne was not coordinated prior to the introduction of H_2.[23] In contrast to the dihydrogen reaction, the initial reaction of **6b** with HCl involved rapid oxidative addition to iridium(I) to give complex **10** and this was followed by slow reductive elimination to give the alkenylplatinum complex **11**. The ^1H NMR spectrum of **10** contained a hydride resonance at δ −19.34 [t, 1H, ^2J(PH) = 14 Hz, ^4J(PtH) = 139 Hz], assigned as an iridium hydride, and the ^{13}C NMR spectrum of a ^{13}CO enriched sample contained resonances for both iridium carbonyl and platinum carbonyl groups at $\delta(^{13}C)$ = 171.2 [s, IrCO] and 178.3 [s, ^1J(PtC) = 1110 Hz, PtCO], respectively. In the ^1H NMR spectrum of **11**, the vinyl protons appeared at δ 5.41 and 5.68, in the range expected for a terminal alkenyl group, and there was a coupling ^3J(HH) = 17 Hz between the two vinyl protons, showing that they are mutually *trans*.[12] The β-hydrogen at δ 5.68 couples to platinum with ^3J(PtH) = 63 Hz, showing that the alkenyl group is bound to platinum. In the ^{13}C NMR spectrum, there was only one carbonyl resonance, assigned as an iridium carbonyl because there was no resolved coupling to platinum. The carbonyl group is terminal, so a bridging chloride ligand is suggested to give a stable structure.[12,14,23,24]

Absorption and emission spectra of complex 6a

The complex $[PtIr(CO)_2(\mu\text{-PhCCH})(\mu\text{-dppm})_2][PF_6]$, **6a**, which is pink in the solid state, forms dichroic solutions which may appear orange (concentrated solution) or bright pink (dilute solution), depending on the concentration and whether viewed by transmitted or reflected light. This unusual colour led us to investigate its absorption and emission spectra (Fig. 5). The UV-visible spectrum of **6a** contains a very weak absorption at 650 nm (ε = 100 M^{-1} cm^{-1}, barely visible in Fig. 5) and a strong absorption at 522 nm (ε = 4.8 × 10^3 M^{-1} cm^{-1}). There are also partially resolved, higher energy, absorptions at *ca.* 420 and 365 nm.

There have been several detailed studies of the photophysical properties of d^8–d^8 face-to-face complexes, for which the two lower energy bands have been assigned, for third row transition metal complexes, as primarily due to the spin forbidden singlet–triplet and spin-allowed singlet–singlet 5dσ*→6pσ transitions.[5,25] Complex **6a** can be considered as a distorted face-to-face complex, because of the constraints of the bridging alkyne ligand, and it has strong π-acceptor carbonyl ligands, so the transitions are likely to be primarily 5dσ*→6pσ/COπ* transitions (Fig. 6). The Pt···Ir bonding should be stronger in the excited state.[25] In the heterobinuclear PtIr complex **6a**, the HOMO will have more iridium $5d_{z^2}$ character and the LUMO will have more platinum $6p_z$ and CO π* character (Fig. 6), so the lowest energy transitions will involve some iridium to platinum charge transfer.[25] The absorption spectrum is very similar to that of the face-to-face Pt(II)Rh(I) complex $[Pt(CN)_2Rh(^tBuNC)_2(\mu\text{-dppm})_2]^+$, **A**, [$\lambda_{max}$ 547 nm (triplet) and 469 (singlet)] except that the bands

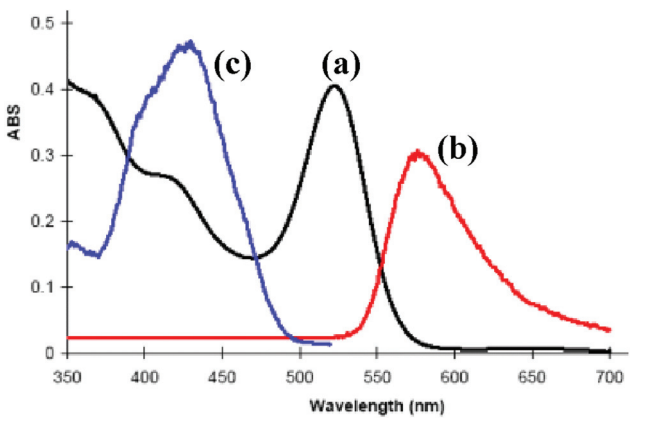

Fig. 5 The photophysical properties of complex **6a** in solution in CH_2Cl_2: (a) absorption spectrum (8.5 × 10^{-5} M); (b) emission spectrum (λ_{ex} = 520 nm); (c) excitation spectrum (λ_{em} = 570 nm).

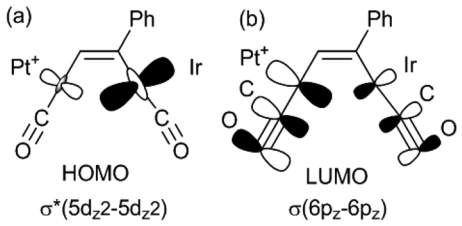

Fig. 6 Schematic diagram of the likely HOMO and LUMO in complexes such as **6a** (dppm ligands omitted for clarity). The different orbital sizes are intended only to depict the likely differences in orbital character in the HOMO and LUMO.

in **6a** are shifted to considerably lower energy [λ_{max} 650 nm (triplet) and 522 (singlet)].[5,25] This shift can be understood in terms of the neutral iridium(I) centre in **6a** being more electron rich than the cationic rhodium(I) centre in **A** and the cationic platinum(II) centre in **6a** being more electron deficient than the neutral platinum(II) centre in **A**.

Complex **6a** is strongly emissive at room temperature in a dichloromethane solution, giving an emission band at 575 nm which is assigned to the 6pσ→5dσ_{z^2}* fluorescence, with a shoulder at *ca.* 670 nm which might arise from the corresponding phosphorescence. The Stokes shift of 53 nm for the main fluorescence band is similar to that observed in related complexes.[5,25] The addition of carbon monoxide to this solution results in the complete suppression of the room temperature luminescence as complex **9a** is formed (Scheme 5).

Computational studies

In order to gain further insight into the above chemistry, DFT calculations were carried out on some of the complexes, using the ligand $CH_2(PMe_2)_2$, dmpm, in place of dppm in order to make the computation times reasonable (see experimental for details).[26] The calculated structures of $[PtIr(CO)_3(\mu\text{-dmpm})_2]^+$, **1***, [Pt–CO 1.96, Ir–CO 1.91, Pt–Ir 2.78 Å, P–Ir–P 175°] and $[PtIrH(CO)_2(\mu\text{-dmpm})_2]$, **2***, [Pt–H 1.64, Ir–CO 1.91, Pt–Ir 2.85 Å, P–Ir–P 156°] are shown in Fig. 7. The structure of complex **1** has been determined [Pt–CO 1.91, Ir–CO 1.90, Pt–Ir 2.77 Å, P–Ir–P 169°] but that of **2** has not. The calculation predicts a greater twist of the diphosphine ligand, a longer Pt–Ir distance and a greater distortion of the P–Ir–P bond angle from linearity in **2** when compared to **1**. These calculated features can be understood in terms of the greater *trans*-influence of hydride in **2** and **2*** compared to carbonyl in **1** and **1***, leading to a higher degree of Pt(II)–Ir(−I) character in **2** and **2***. Note that the complexes can be formulated as Pt(0)–$Ir(I)^+$, $Pt(I)^+$–Ir(0) or $Pt(II)^{2+}$–$Ir(-I)^-$, depending on how the electrons in the PtIr bond are assigned.[27] The HOMO in both **1** and **2** is expected to be Pt–Ir bonding, with a high degree of iridium 6p/5d character, Fig. 7, and the calculation for **1*** and **2*** predicts polarity $Pt^{\delta+}$–$Ir^{\delta-}$ [calculated Hirshfeld charges: **1***, Pt 0.03e, Ir −0.17e; **2***, Pt −0.08e, Ir −0.22e]. Oxidation of both **1** and **2** is expected to occur at the more electron-rich iridium centre, provided there is a low energy pathway.

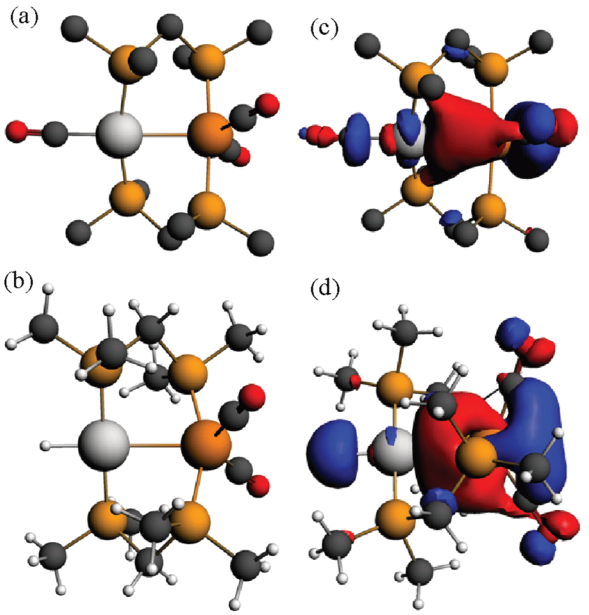

Fig. 7 The calculated structure of (a) $[PtIr(CO)_3(\mu\text{-dmpm})_2]^+$, **1***, [Pt–CO 1.96, Ir–CO 1.91, Pt–Ir 2.78 Å, P–Ir–P 175°] and (b) $PtIrH(CO)_2(\mu\text{-dmpm})_2]$, **2***, [Pt–H 1.64, Ir–CO 1.91, Pt–Ir 2.85 Å, P–Ir–P 156°] with (c) and (d) the corresponding HOMO.

Calculations were carried out on the isomers of the model complex cation $[PtIrH_4(CO)(\mu\text{-dmpm})_2]^+$, **3***, which is a model for the complex **3** formed by reaction of dihydrogen with complex **1** (Schemes 2 and 3). Good minima were found for isomers **3a*** and **3b*** (Fig. 8), but attempts to optimize the geometry of isomers **3c*** or **3d*** (or isomers with only terminal hydrides) led to spontaneous isomerisation to **3b***. A plausible reaction coordinate diagram for the fluxionality of complex **3** based on these calculations and on the experimental observations (Fig. 1, Scheme 3) is shown in Fig. 8. The high point is the transition state associated with inversion of the PtHIr group in **3d***, and this is the step that leads to H^c–H^d exchange.

The calculated structure of the complex $[PtIrH(SiMePh_2)(CO)_2(\mu\text{-dmpm})_2]^+$, **5***, as a model for the dppm analogue **5** (Scheme 2), is shown in Fig. 9. The structure is rigid with a highly twisted $PtIr(\mu\text{-dmpm})_2$ unit, as a result of the steric effects of the silyl group. The corresponding complex $[PtIrH_2(CO)_2(\mu\text{-dmpm})_2]^+$, **12***, was also studied as a model for the first step in the oxidative addition of dihydrogen to complex **1**. In this case, the isomer **12a***, which is analogous to **5***, was predicted to be the most stable isomer but the complex is much more flexible than **5*** and isomers with a bridging hydride, such as **12b*** (ΔE +63 kJ mol^{-1} from **12a***) or with one hydride transferred to platinum, such as **12c*** (ΔE +76 kJ mol^{-1} from **12a***), are predicted to be kinetically accessible (Fig. 9).

Several mechanisms can therefore be considered possible for a second oxidative addition of dihydrogen to $[PtIrH_2(CO)_2(\mu\text{-dppm})_2]^+$, **12**, to give complex **3** (Scheme 2). In isomer **12a** the iridium centre has an 18-electron configur-

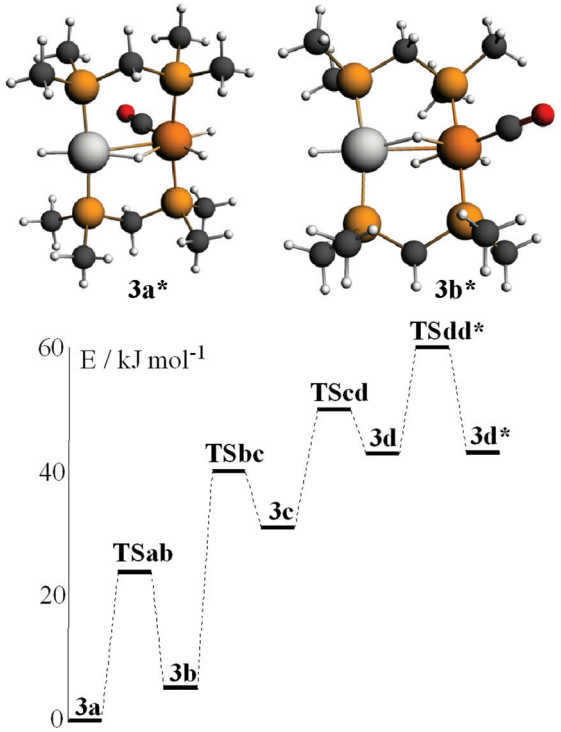

Fig. 8 The calculated structures of isomers **3a*** and **3b*** of $[PtIrH_4(CO)(\mu\text{-dmpm})_2]^+$ and a plausible reaction coordinate diagram for the observed fluxionality of the dppm analogue (Scheme 3).

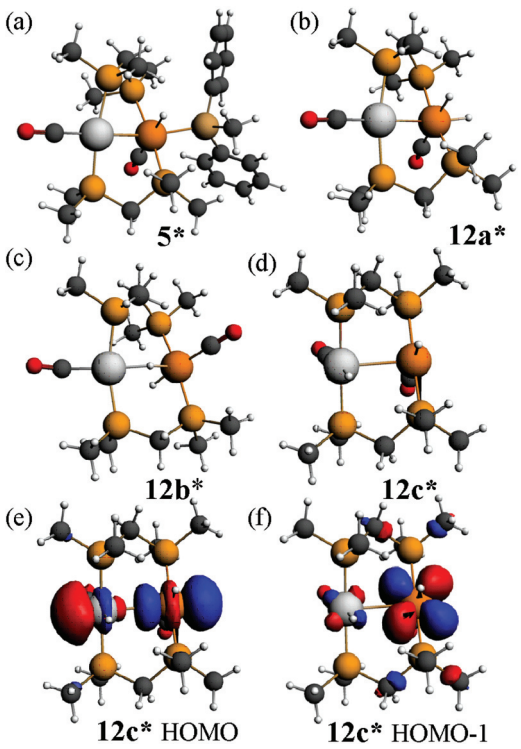

Fig. 9 The calculated structures of (a) the complex $[PtIrH(SiMePh_2)(CO)_2(\mu\text{-dmpm})_2]^+$, **5***, (b), (c), (d) possible isomers of $[PtIrH_2(CO)_2(\mu\text{-dmpm})_2]^+$, **12***, and (e), (f) the highest energy 5dσ* and 5dπ* occupied MOs of the face-to-face isomer **12c***.

ation, so concerted oxidative addition would occur either at platinum or across the Pt–Ir bond. However, the face-to-face isomer **12c** contains a 16-electron iridium(I) centre, and the highest occupied molecular orbitals have mostly iridium 5d character, so oxidative addition might occur at iridium after isomerisation of **12a** to **12c**. The carbonyl dissociation from platinum might occur during or after the oxidative addition of dihydrogen.

Calculated structures of some isomers of $[PtIrH_2Cl_2(CO)(\mu\text{-dmpm})_2]^+$, **4***, are shown in Fig. 10. The most stable isomer is **4c***, followed by **4d***, **4a*** and **4b***, with isomers having the iridium chloride ligand *trans* to the Pt–Ir bond at higher energy. Complexes **4a*** and **4b***, and **4c*** and **4d***, can interconvert by inversion of the PtHIr group, but there is no easy way for **4a*** to isomerise to **4c***. The NMR spectra of the complex $[PtIrH_2Cl_2(CO)(\mu\text{-dppm})_2]^+$, **4**, were considered to favour isomer **4a**, but the evidence is not definitive and a structure analogous to **4c*** cannot be ruled out. The calculations support the presence of a very unsymmetrical bridging hydride (Fig. 10), with a short Pt–H and a long Ir···H distance, as suggested by the hydride NMR data.

Some calculated structures for the dmpm analogues of alkyne complexes **6** and **8** (Scheme 3) are shown in Fig. 11 and 12.

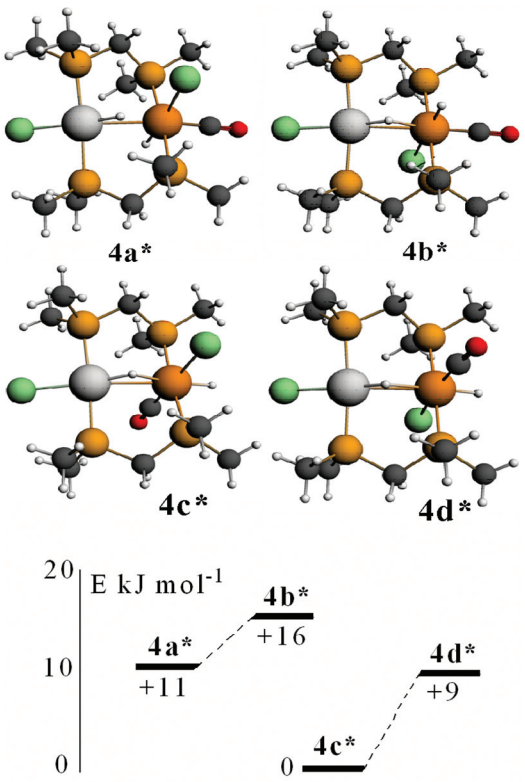

Fig. 10 The calculated structures of some isomers of $[PtIrH_2Cl_2(CO)(\mu\text{-dmpm})_2]^+$, **4***, and their relative energies. Selected calculated distances: **4a***, Pt–H 1.66, Ir···μ-H 1.92, Ir–H 1.62, Ir–CO 1.88, Pt···Ir 2.85 Å; **4b***, Pt–H 1.67, Ir···μ-H 1.89, Ir–H 1.62, Ir–CO 1.88, Pt···Ir 2.86 Å; **4c***, Pt–H 1.65, Ir···μ-H 1.95, Ir–H 1.61, Ir–CO 1.87, Pt···Ir 2.93 Å; **4d***, Pt–H 1.64, Ir···μ-H 2.00, Ir–H 1.61, Ir–CO 1.87, Pt···Ir 2.91 Å.

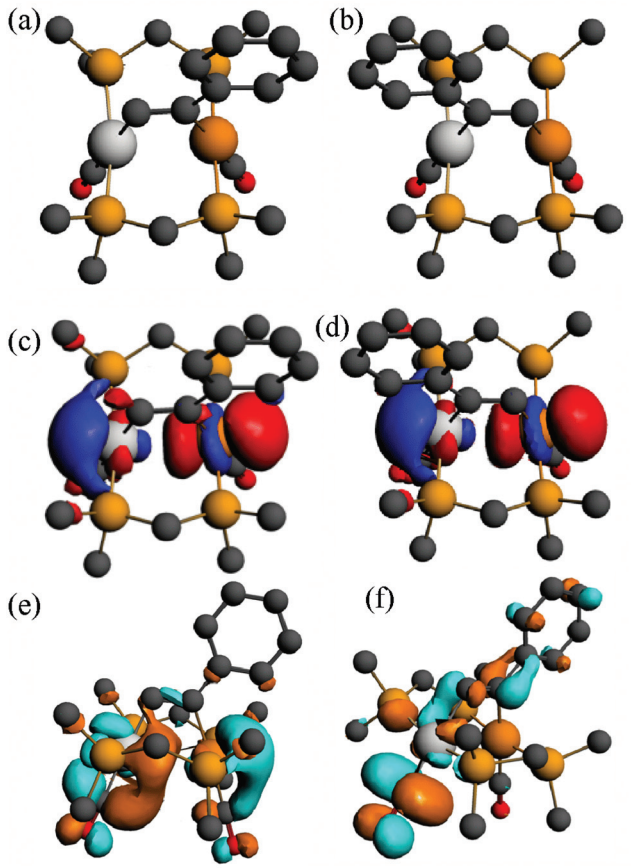

Fig. 11 (a), (b) The calculated structures of the alkyne complex [PtIr(HCCPh)(CO)$_2$(μ-dmpm)$_2$]$^+$, **6a***, and its isomer **6a*′**, (c), (d) the HOMO for **6a*** and **6a*′**, (e), (f) the LUMO and LUMO+1 for **6a***.

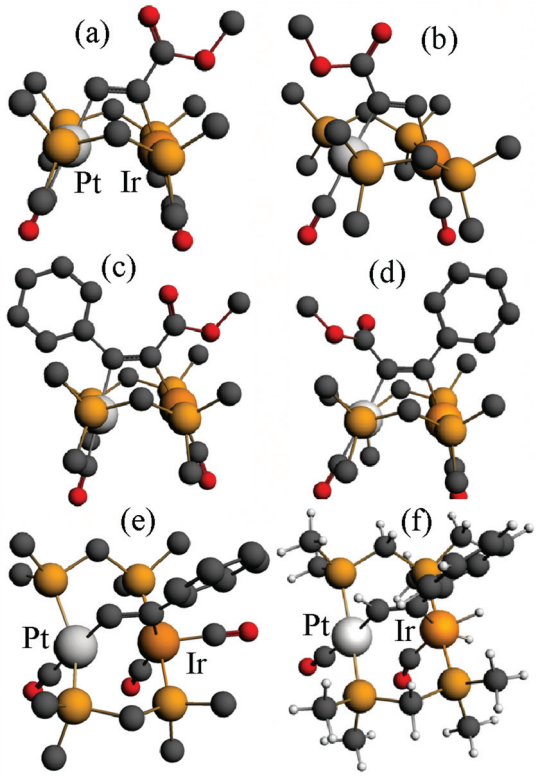

Fig. 12 (a), (b) The calculated structures of the alkyne complex [PtIr(HCCCO$_2$Me)(CO)$_2$(μ-dmpm)$_2$]$^+$, **6c*** and its isomer **6c*′**, (c), (d) complex **8a*** and its isomer **8b***, (e) complex **9a**, (f) the possible intermediate dihydride complex **13***.

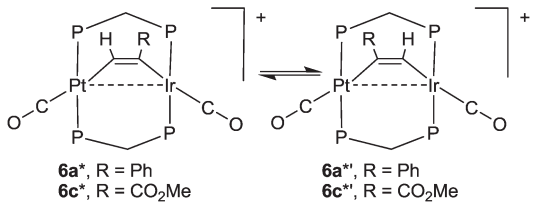

Scheme 7 Predicted equilibrium between isomers of the alkyne complexes **6** (PP = dmpm).

The calculated energies of reaction to form the alkyne complexes **6a***, **6c***, **7*** and **8a*** from complex **1***, with displacement of one carbonyl ligand are −22, −85, −99 and −72 kJ mol^{-1} respectively, predicting that more electronegative substituents on the alkyne, and especially the –CO$_2$Me groups, favour the reaction. For the complex **6a*** or **6c*** the conformation of the phenyl or –CO$_2$Me group respectively is close to coplanar with the Pt–C═C–Ir unit, which allows maximum π-conjugation, but in the disubstituted alkyne complex **8a*** or **8b*** the substituents are twisted out of the Pt–C═C–Ir plane to reduce steric effects (Fig. 12). The reduction in π-bonding because of this twisting effect can explain the lack of reactivity of diphenylacetylene with complex **1** (the calculated energy of reaction is −13 kJ mol^{-1}). The calculation predicts that **8a** is more stable than **8b**, but by only 4 kJ mol^{-1}, consistent with the experimental observation that both isomers are formed. However, the calculations predict that, based on the ground state energies, there might also be an equilibrium between the isomers **6a*** and **6a*′** [**6a*′** favoured by 4 kJ mol^{-1}] and between **6c*** and **6c*′** [**6c*′** favoured by 3 kJ mol^{-1}] (Scheme 7) whereas, experimentally, only isomers **6a** and **6c** were observed (Scheme 4). No significant differences between steric effects in the isomers are expected. Unless the calculations give a wrong prediction, it is likely that the observed selectivity is based on kinetic rather than thermodynamic control. Perhaps the alkyne first coordinates to iridium with the bulky substituent oriented outwards, then slides over to the bridging position. Fig. 12e shows the calculated structure of [PtIr(μ-HCCPh)(CO)$_3$(μ-dmpm)$_2$]$^+$, **9a***, which is a model for the complex **9a**, observed on the initial reaction of **6a** with CO (Scheme 5). Complex **9a** might also be an intermediate in the reaction of phenylacetylene with complex **1**. Dihydrogen is also expected to react with **6a** at the iridium centre, and the structure of a potential dihydride complex [PtIrH$_2$(μ-HCCPh)(CO)$_2$(μ-dmpm)$_2$]$^+$, **13a***, is shown in Fig. 12f. Initial C–H reductive elimination from an analogous intermediate [PtIrH$_2$(μ-HCCPh)(CO)$_2$(μ-dmpm)$_2$]$^+$, **13a**, would give a styrenyl complex, related to the observed complex **11** (Scheme 6), and a

further oxidative addition of hydrogen and C–H reductive elimination would give styrene. However, given the ease with which hydride and carbonyl ligands can migrate between metal centres, there are several mechanisms that might apply.

The absorption and emission spectra of complex **6a** can be understood in terms of the frontier orbitals for the model complex **6a*** shown in Fig. 11. The HOMO (Fig. 11c) is primarily the Pt–Ir 5dσ* molecular orbital, which is similar to that in the face-to-face complex **12c*** (Fig. 9e), though the planes of the platinum(II) and iridium(I) are at an angle from the ideal face-to-face orientation. This HOMO has a greater character of the more electron rich iridium(I) centre, and it is very similar to that calculated for the isomeric **6a*′** (Fig. 11d). The LUMO has mostly Pt–Ir $6p_z$ bonding character, with significant contribution of the p_z–π* character of the carbonyl ligands, and is mostly centred on the PtCO group. The lowest energy singlet–singlet absorption and emission bands for **6a** (Fig. 5) are associated with the transition between these molecular orbitals, in agreement with literature assignments for related compounds.[5,25] The first singlet–singlet absorption band for complex **6a*** is calculated to have a maximum at 537 nm, compared to the observed band for **6a** at 522 nm.

Conclusions

The metal oxidation states in complex **1** can be considered as Pt(0)–Ir(I)$^+$, Pt(I)$^+$–Ir(0) or Pt(II)$^{2+}$–Ir(−I)$^-$, depending on how the electrons in the PtIr bond are assigned, but the reactivity is most easily interpreted in terms of the Pt(II)$^{2+}$–Ir(−I)$^-$ formalism, in which the metal–metal bond can be considered as a donor–acceptor bond, formed by donation of electrons from Ir(−I) to Pt(II).[27] This is also consistent with the nature of the HOMO (Fig. 7) and with the calculated charges on platinum and iridium in **1***. Thus the nucleophilic substitution of hydride for carbonyl in **1** occurs at the platinum centre, while oxidative addition reactions occur, at least initially, at the iridium centre (Scheme 2). Alkynes react with **1** at the metal–metal bond and the products **6–8** (Scheme 4) are considered as distorted face-to-face Pt(II)···Ir(I) complexes, and complex **6a** exhibits strong room temperature emission, which is a characteristic property of such complexes.[5]

The unusual chemistry of the polar Pt–Ir bond in complex **1** may provide insight into the mechanisms of reaction of the important bimetallic PtIr catalysts.[3,4]

Experimental

The syntheses were carried out using standard Schlenk techniques under an atmosphere of nitrogen. The complex [PtIr(CO)$_3$(μ-dppm)$_2$][PF$_6$], **1**, was prepared by the literature method, from [Pt(η^2-dppm)$_2$][PF$_6$]$_2$ and [PPN][Ir(CO)$_4$], and ^{13}CO enriched samples were prepared by stirring under an atmosphere of ^{13}CO.[6,28] The ^{1}H, ^{31}P{^{1}H}, and ^{13}C{^{1}H} NMR spectra were recorded using a Varian Gemini 300, Varian Inova 400 or Inova 600 spectrometer. The gCOSY, gHSQC, and gHMBC spectra were recorded using the Varian Inova 400 or Inova 600 spectrometer. Chemical shifts are cited with respect to TMS or 85% phosphoric acid (^{31}P). IR spectra were recorded with Nujol mulls or solutions using a Perkin Elmer 2000 FTIR spectrometer. Emission spectra were recorded by using a Fluorolog-3 spectrofluorimeter (ISA Jobin Yvon Spex), using a solution in CH_2Cl_2 at room temperature in a quartz cuvette. DFT calculations (gas phase only) were carried out by using the Amsterdam Density Functional (ADF) program based on the BP functional, with double-zeta basis set and first-order scalar relativistic corrections.[26]

X-ray crystallography[29]

Crystals of compounds **6a**, **6b**, and **6c** were mounted on glass fibers. Programs for diffractometer operation, data collection, cell indexing, data reduction and absorption correction were those supplied by Nonius. Diffraction measurements were made using a Nonius Kappa-CCD diffractometer using graphite-monochromated Mo-Kα radiation at 200 K (**6a** and **6c**) or 150 K (**6b**). Structure solution and refinement was carried out using the SHELX97 or the SHELXT suite of programs, using the WinGX graphical interface. The initial solutions were obtained by direct methods and refined by successive least-squares cycles. Compound **6a** co-crystallized with two solvent acetone molecules, one of which was disordered over two positions, as was the PF_6^- counterion. All non-hydrogen atoms in the main residue were refined anisotropically. Disordered C, O, and F atoms in the disordered solvent and anion were refined isotropically. The agreement factors were poor and so this is considered as a partial structure determination only. Compound **6b** co-crystallized with a small amount of a chloro analog, presumably formed from the CH_2Cl_2 solvent during crystallization. The resulting CO–Cl (75 : 25) disorder was successfully modeled and all non-H atoms were refined anisotropically. Compound **6c** was refined as a racemic twin, and also contains disorder in the CO_2CH_3 group of the main residue, as well as in two phenyl rings of the main residue. In each case, the disorder was modelled over two positions using isotropic thermal parameters for the disordered C and O positions. All other non-H atoms in the main residue were refined anisotropically. Disorder was also present in the PF_6^- counterion and in two co-crystallized CH_2Cl_2 molecules. Details of the data collection and refinement can be found in the cif files (CCDC 1040457–1040458).

[HPt(μ-dppm)$_2$Ir(CO)$_2$], 2

To a stirred solution of [(CO)Pt(μ-dppm)$_2$Ir(CO)$_2$][PF$_6$] (35 mg) in thf (10 mL) was added a solution of NaBHEt$_3$ in thf (1.0 mL, 2 M). The solution was vigorously stirred for 3 hours, over which time the orange colour of the solution changed to yellow colour. The solvent was removed under vacuum, the solid was extracted with CH_2Cl_2 (1 mL) and the product was precipitated as a yellow solid by addition of pentane (5 mL). Yield: 17 mg, 55%. Anal. Calc. for $C_{52}H_{45}IrO_2P_4Pt$: C, 51.48; H, 3.74. Found: C, 50.97; H, 3.53%. NMR in CD_2Cl_2: $\delta(^1H)$ = −3.33

[m, 1H, ^1J(PtH) = 1123 Hz, PtH], 4.85 [br t, 4H, ^2J(PH) = 4 Hz, CH_2], 7.0–7.8 [m, 40H, Ph]; $\delta(^{31}P)$ = 16.08 [t, J(PP) = 30 Hz, ^1J(PtP) = 2873 Hz, PtP]; −16.40 [t, J(PP) = 30 Hz, ^2J(PtP) = 69 Hz, IrP].

[HPt(μ-dppm)$_2$(μ-H)Ir(H)$_2$(CO)][PF$_6$], 3

To a stirred, degassed solution of [PtIr(CO)$_3$(μ-dppm)$_2$][PF$_6$] (30 mg) in CH_2Cl_2 (10 mL) was added dihydrogen (1 atm) and the flask was sealed. The colour slowly changed from orange to yellow. After 3 h, the solvent was removed under vacuum, the residue was redissolved in a minimum amount of CH_2Cl_2 (*ca.* 1 mL) and the product was precipitated as a yellow solid by addition of ether (5 mL). Yield: 25 mg, 82%. Anal. Calc. for $C_{51}H_{48}F_6IrOP_5Pt$: C, 45.95; H, 3.63. Found: C, 45.49; H, 3.55%. IR (Nujol): ν(CO) = 2080 cm^{-1} (s). NMR in CD_2Cl_2 at −30 °C: $\delta(^1H)$ = −12.02 [br s, 1H, ^3J(PtH) 90 Hz, IrH^d], −9.52 [br s, 1H, ^1J(PtH) 540 Hz, PtH^{b}Ir], −8.17 [m, 1H, ^2J(PH) 15 Hz, IrH^c], −3.90 [m, 1H, ^2J(PH) 15 Hz, ^1J(PtH) 1225 Hz, PtH^a], 3.88 [m, 2H, CH_2P_2], 5.23 [m, 2H, ^3J(PtH) 55 Hz, CH_2P_2], 7.0–8.0 [m, 40H, Ph]; $\delta(^{31}P)$ = 19.61 [m, J(PP) = 36 Hz, ^1J(PtP) = 2817 Hz, PtP], −1.60 [t, J(PP) = 36 Hz, IrP], −143.42 [septet, ^1J(PF) = 711 Hz, PF_6].

[HClPt(μ-dppm)$_2$IrHCl(CO)][PF$_6$], 4

To a solution of [(CO)Pt(μ-dppm)$_2$Ir(CO)$_2$][PF$_6$] (127.5 mg, 0.0919 mmol) in CH_2Cl_2 (10 mL) was added a solution of HCl in CH_2Cl_2 (10 mL, 0.09 M). Immediately upon addition, effervescence was noted and the colour of the solution changed from orange to yellow. The solvent was removed *in vacuo* and the residue recrystallized from CH_2Cl_2–ether to give a pale yellow solid. Yield: 88 mg, 78%. Anal. Calc. for $C_{51}H_{46}Cl_2F_6IrOP_5Pt$: C, 43.69; H, 3.31. Found: C, 43.25; H, 3.08%. IR: ν(CO) = 2048 cm^{-1} (s). NMR in CD_2Cl_2: $\delta(^1H)$ = −15.53 [s, 1H, ^1J(PtH) = 858 Hz, PtH]; −15.02 [t, 1H, ^2J(PH) = 10 Hz, IrH]; 4.52 [m, 2H, CH_2P_2]; 4.78 [m, 2H, CH_2P_2]; 7.2–7.8 [m, 40H, Ph]; $\delta(^{31}P)$ = 7.84 [t, J(PP) = 34 Hz, ^1J(PtP) = 2344 Hz, PtP]; −6.28 [m, J(PP) = 34 Hz, IrP]; −143.3 [septet, ^1J(PF) = 711 Hz, PF_6]; $\delta(^{13}C)$ = 159.99 [m, ^2J(PtC) = 180 Hz, IrCO].

[(CO)Pt(μ-dppm)$_2$IrH(CO)(SiPh$_2$Me)][PF$_6$], 5

To a stirred solution of [(CO)Pt(μ-dppm)$_2$Ir(CO)$_2$][PF$_6$] (61.1 mg, 0.441 mmol) in CH_2Cl_2 (10 mL) was added diphenylmethylsilane (0.2 g, 1 mmol). The colour of the solution slowly changed from orange to yellow. After 24 h, the solvent was removed *in vacuo* and the residue was recrystallized from CH_2Cl_2–ether. Yield: 46 mg, 67%. Anal. Calc. for $C_{65}H_{58}F_6IrO_2P_5PtSi$: C, 51.12; H, 3.83. Found: C, 50.63; H, 3.77%. IR: ν(CO) = 2046 cm^{-1} (s), 1945 cm^{-1} (m). NMR in CD_2Cl_2: $\delta(^1H)$ = −8.29 [t, 1H, ^2J(PH) = 14 Hz, ^2J(PtH) = 33 Hz, IrH]; 0.42 [s, 3H, ^2J(SiH) = 40 Hz, SiMe]; 5.07 [m, 2H, CH_2P_2]; 6.12 [m, 2H, CH_2P_2]; 6.4–8.2 [m, 52H, Ph]; $\delta(^{13}C)$ = 186.83 [m, ^2J(PC) = 10 Hz, ^2J(HC) = 32 Hz, IrCO]; 170.08 [m, ^1J(PtC) = 1130 Hz, PtCO]; $\delta(^{29}Si)$ = −10.0; $\delta(^{31}P)$ = −3.64 [m, J(PP) = 40 Hz, ^2J(PPtP) = 350 Hz, ^1J(PtP) = 2946 Hz, PtP]; −6.16 [m, J(PP) = 40 Hz, ^2J(PPtP) = 350 Hz, ^1J(PtP) = 3032 Hz, PtP]; −20.84, −20.86 [m, IrP]; −143.39 [septet, ^1J(PF) = 710 Hz, PF_6].

[PtIr(CO)$_2$(μ-HCCPh)(μ-dppm)$_2$][PF$_6$], 6a

To a solution of [PtIr(CO)$_3$(μ-dppm)$_2$][PF$_6$], **1**, (50 mg, 0.036 mmol) in CH_2Cl_2 (10 mL) was added phenylacetylene (3.7 mg, 3.9 μL, 0.072 mmol) and the mixture was stirred under nitrogen for 16 h. Over the reaction time, a change from an orange solution to a bright pink/orange dichroic solution was observed. The solvent was removed *in vacuo* and the pink residue was recrystallized from CH_2Cl_2–Et_2O to yield the product as a dark pink solid. Yield: 35 mg, 68%. Anal. Calc. for $C_{60}H_{50}F_6IrO_2P_5Pt$: C, 49.39; H, 3.45. Found: C, 49.47; H, 3.45%. IR(Nujol): ν(CO) = 2067 (m), 1964 (s); ν(CC) = 1606 (s). NMR in CD_2Cl_2: $\delta(^1H)$ = 3.79 [m, 2H, ^2J(HH) = 14 Hz, ^3J(PH) = 7 Hz, CH_2P_2], 4.31 [m, 2H, ^3J(PtH) = 60 Hz, CH_2P_2], 6.42 [d, 2H, ^3J(HH) = 7 Hz, Ph H^o], 6.59 [t, 2H, ^3J(HH) = 7 Hz, Ph H^m], 6.72 [t, 1H, ^3J(HH) = 7 Hz, Ph H^p], 7.04 [tt, 1H, ^3J(PH) = 14 Hz, ^4J(PH) = 1 Hz, PhCC*H*], 7.2–7.8 [m, 40H, dppm Ph]; $\delta(^{31}P)$ = 16.5 [m, IrP], 3.8 [m, ^1J(PtP) = 1630 Hz, PtP]; $\delta(^{13}C)$ = 17.7 [m, CH_2P_2]; 119.2 [s, ^1J(PtC) = 820, Pt*C*CIr], 129.9 [t, ^2J(PC) = 25 Hz, PtC*C*Ir], 129.0–134.3 [Ph], 177 [t, ^2J(PC) = 10 Hz, Ir*C*O], 184 [t, ^2J(PC) = 8 Hz, ^1J(PtC) = 1105 Hz, Pt*C*O].

[PtIr(CO)$_2$(μ-HCC-4-C$_6$H$_4$Me)(μ-dppm)$_2$][PF$_6$], 6b

This was prepared in a similar way from complex **1** (29.8 mg, 0.022 mmol) and 4-ethynyltoluene (4 μL, 0.032 mmol). Yield: 24.7 mg, 84%. Anal. Calc. for $C_{61}H_{52}F_6IrO_2P_5Pt$: C, 49.73; H, 3.56. Found: C, 49.38; H, 3.47%. IR (Nujol): ν(CO) = 2065 m, 1954 m. NMR in CD_2Cl_2: $\delta(^1H)$ = 2.00 [s, 3H, Me], 3.25 [m, CH_2P_2], 3.75 [m, CH_2P_2], 6.28 [d, 2H, ^3J(HH) = 8 Hz, C_6H_4–H^o], 6.37 [d, 2H, ^3J(HH) = 8 Hz, C_6H_4–H^m], 6.97 [tt, 1H, ^3J(PH) = 14 Hz, ^4J(PH) = 2 Hz, C═CH], 7.10–7.70 [m, 40H, Ph]; $\delta(^{31}P)$ = 16.19 [m, IrP]; 2.83 [m, ^1J(PtP) = 3236 Hz, PtP]; −142.2 [septet, ^1J(PF) = 710 Hz, PF_6]; $\delta(^{13}C)$ = 18.0 [m, CH_2], 20.9 [s, Me], 119.2 [m, C═*C*H], 128–134 [m, Ph], 183.88 [t, ^2J(PC) = 8 Hz, ^1J(PtC) = 1117 Hz, PtCO]; 188.65 [t, ^2J(PC) = 10 Hz, IrCO].

[PtIr(CO)$_2$(μ-HCCCO$_2$Me)(μ-dppm)$_2$][PF$_6$], 6c

This was prepared in a similar way from complex **1** (71.9 mg, 0.0519 mmol) and methyl propiolate (4.7 μL, 0.0528 mmol). Yield: 51.1 mg, 68%. Anal. Calc. for $C_{56}H_{48}F_6IrO_4P_5Pt$: C, 46.67; H, 3.36. Found: C, 46.65; H, 3.01%. IR(Nujol): ν(CO) = 2064 (m), 1959 (m); ν(CO) of CO_2CH_3 = 1687 (m). NMR in CD_2Cl_2: $\delta(^1H)$ = 2.63 [s, 3H, Me], 3.60 [m, 2H, CH_2P_2], 3.84 [m, 2H, CH_2P_2], 7.0–8.1 [m, 40H, Ph]; $\delta(^{31}P)$ = 12.95 [m, IrP]; 2.45 [m, ^1J(PtP) = 3105 Hz, PtP]; −143.36 [septet, ^1J(PF) = 710 Hz, PF_6].

[PtIr(CO)$_2$(μ-MeO$_2$CCCCO$_2$Me)(μ-dppm)$_2$][PF$_6$], 7

This was prepared in a similar way from complex **1** (176 mg, 0.1271 mmol) and dimethyl acetylenedicarboxylate (16 μL, 0.130 mmol). Yield: 140 mg, 73%. Anal. Calc. for $C_{58}H_{50}F_6IrO_6P_5Pt$: C, 46.47; H, 3.36. Found: C, 45.98; H, 3.22%. IR(Nujol): ν(CO) = 2043 (m), 1952 (m); ν(CO) of CO_2CH_3 = 1702 (m). NMR in CD_2Cl_2: $\delta(^1H)$ = 2.20 [s, 3H, OMe], 2.47 [s, 3H, OMe], 3.75 [m, 2H, CH_2P_2], 3.88 [m, 2H, CH_2P_2], 7.1–8.3 [m, 40H, Ph]; $\delta(^{31}P)$ = 8.30 [m, IrP]; 0.12 [m, ^1J(PtP) = 2862 Hz,

PtP]; −143.39 [septet, ^1J(PF) = 710 Hz, PF_6]; $\delta(^{13}C)$ = 178.86 [t, ^2J(PC) = 10 Hz, ^1J(PtC) = 1096 Hz, PtCO]; 187.72 [t, ^2J(PC) = 9 Hz, IrCO].

[PtIr(CO)$_2$(μ-PhCCCO$_2$Me)(μ-dppm)$_2$][PF$_6$], 8a and 8b

This was prepared in a similar way from complex **1** (71.7 mg, 0.0518 mmol) and methyl phenylpropiolate (8.3 μL). Yield: 47 mg, 60%. Anal. Calc. for $C_{62}H_{52}F_6IrO_4P_5Pt$: C, 49.08; H, 3.45. Found: C, 49.26; H, 3.41%. IR(Nujol): ν(CO) = 2059 (m), 1948 (m); ν(CO) of CO_2CH_3 = 1698 (m). NMR in CD_2Cl_2: $\delta(^1H)$ = 2.26 [s, OMe], 2.35 [s, OMe], 3.80 [m, CH_2P_2], 3.80 [m, CH_2P_2], 3.92 [m, CH_2P_2], 3.97 [m, CH_2P_2], 4.07 [m, CH_2P_2], 5.95–8.00 [m, Ph]; $\delta(^{31}P)$ = 9.02 [m, IrP]; 7.97 [m, IrP]; −0.28 [m, ^1J(PtP) = 2995 Hz, PtP]; −1.54 [m, ^1J(PtP) = 2887 Hz, PtP]; −143.37 [septet, ^1J(PF) = 710 Hz, PF_6]. It was not possible to assign resonances to specific isomers because they were formed in equal amounts.

Reaction of 6a and 6b with CO to give [PtIr(CO)$_3$(μ-RCCH)-(μ-dppm)$_2$][PF$_6$], 9a and 9b

An NMR tube containing a solution of complex **6b** (29.5 mg, 0.020 mmol) in CD_2Cl_2 (1 mL) was cooled to −80 °C and then evacuated and refilled with ^{13}CO. On shaking the tube, the colour of the solution changed from pink/orange to yellow, and spectra were recorded at −30 °C and at 20 °C. NMR in CD_2Cl_2 for **9b**: $\delta(^1H)$ = 2.18 [s, 3H, Me], 3.73 [m, 2H, CH_2P_2], 3.87 [m, 2H, CH_2P_2], 6.19 [d, 2H, ^3J(HH) = 8 Hz, C_6H_4–H^o], 6.73 [d, 2H ^3J(HH) = 8 Hz, C_6H_4–H^m], 7.1–7.7 [m, 41H, Ph and =CH]; $\delta(^{13}C)$ = 20.1 [s, Me], 126.0 [C_6H_4–C^o], 128.8 [C_6H_4–C^m], 128–135 [Ph], 175.67 [m, IrCO], 178. 35 [m, IrCO], 184.80 [s, ^1J(PtC) = 1184 Hz, PtCO]; $\delta(^{31}P)$ = 5.78 [m, ^1J(PtP) = 3164 Hz, PtP]; −4.42 [s, IrP]; −143.31 [septet, ^1J(PF) = 711 Hz, PF_6]. At 20 °C, resonances for **9b** were still observed, but there were also resonances for complex **1** and MeC_6H_4CCH. The IrP (δ −3.96) and IrCO (δ 176) resonances were broad. When the CO was removed, the resonances for **6b** returned.

The reaction of CO with **6a** was carried out in a similar way to give reversible formation of **9a**. NMR in CD_2Cl_2: $\delta(^1H)$ = 3.81 [m, 2H, CH_2P_2], 3.93 [m, 2H, CH_2P_2], 6.32 [m, 2H, C_6H_5–H^o], 6.91[m, 2H, C_6H_5–H^m], 7.04 [m, 1H, C_6H_5–H^p], 7.2–7.8 [m, 41H, Ph and =CH]; $\delta(^{13}C)$ = 182 [br, IrCO], 184.7 [s, ^1J(PtC) = 1176 Hz, PtCO]; $\delta(^{31}P)$ = 5.5 [m, ^1J(PtP) = 3170 Hz, PtP], −4 [br, IrP].

Reaction of 6b with dihydrogen

A solution of complex **6b** (74 mg, 0.050 mmol) in CD_2Cl_2 (1 mL) in an NMR tube was treated with hydrogen (1 atmos.). The colour of the solution changed from pink-orange to orange over a period of 48 h., and NMR spectra were recorded during this period. Resonances for **6b** decayed to zero after 48 h and were replaced by those for complex **3** (data as above) and 4-$MeC_6H_4CH{=}CH_2$, which were identical to those of an authentic sample. No resonances for 4-MeC_6H_4CCH were observed. The product **3** was precipitated by addition of pentane. Yield: 45 mg, 67%.

[PtIrHCl(CO)$_2$(μ-dppm)$_2$(μ-HC=C-4-C$_6$H$_4$Me][PF$_6$], 10, and [PtIr(μ-Cl)(CH=CH-4-C$_6$H$_4$Me)(CO)(μ-dppm)$_2$][PF$_6$], 11

To a solution of complex **6b** (72.2 mg, 0.049 mmol) in CD_2Cl_2 (0.6 mL) in an NMR tube was added a solution of HCl in CD_2Cl_2 (0.42 mL, 0.12 M, 0.0504 mmol). There was an immediate colour change from pink to orange. The initial product **10** was characterized spectroscopically. NMR in CD_2Cl_2: $\delta(^1H)$ = −19.34 [t, 1H, ^2J(PH) = 14 Hz, ^4J(PtH) = 139 Hz, IrH], 2.00 [s, 3H, Me], 3.33 [m, 2H, CH_2P_2], 3.62 [m, 2H, CH_2P_2], 6.09 [d, 2H, ^3J(HH) = 8 Hz, C_6H_4–H^o], 6.23 [d, 2H, ^3J(HH) = 8 Hz, C_6H_4–H^m], 6.70 [m, 1H, C=CH], 7.0–7.9 [m, 40H, Ph]; $\delta(^{13}C)$ = 171.2 [s, IrCO], 178.3 [s, ^1J(PtC) = 1110 Hz, PtCO]; $\delta(^{31}P)$ = 12.89 [t, ^2J(PP) = 22 Hz, ^1J(PtP) = 2398 Hz, PtP]; −9.09 [m, IrP]; −143.31 [septet, ^1J(PF) = 711 Hz, PF_6]. After 17 h., the conversion to complex **11** was complete, and the product was isolated by evaporation of the solvent and precipitation from a solution in CH_2Cl_2 by addition of pentane. Yield: 54%. Anal. Calc. for $C_{60}H_{53}ClF_6IrOP_5Pt$: C, 48.64; H, 3.61. Found: C, 48.22; H, 3.46%. IR(Nujol) ν(CO) = 1996 cm^{-1}. NMR in CD_2Cl_2: $\delta(^1H)$ = 2.06 [s, 3H, Me], 4.24 [m, 2H, CH_2P_2], 4.55 [m, 2H, CH_2P_2], 5.41 [dt, 1H, ^3J(HH) = 17 Hz, ^3J(PH) = 7 Hz, Pt–CH=C], 5.68 [d, 1H, ^3J(HH) = 17 Hz, ^3J(PtH) = 63 Hz, PtC=CH], 5.88 [d, ^3J(HH) = 8 Hz, C_6H_4–H^o], 6.63 [d, ^3J(HH) = 8 Hz, C_6H_4–H^m], 6.8–8.2 [m, 40H, Ph]; $\delta(^{13}C)$ = 171.13 [s, IrCO]; $\delta(^{31}P)$ = 17.50 [m, ^1J(PtP) = 2858 Hz, PtP]; −5.00 [s, br, IrP]; −143.34 [septet, ^1J(PF) = 711 Hz, PF_6].

Acknowledgements

We thank the NSERC (Canada) for financial support.

Notes and references

1 K. Wade, *J. Chem. Soc., Chem. Commun.*, 1971, 792; K. Wade, *Inorg. Nucl. Chem. Lett.*, 1972, **8**, 559; K. Wade, *Chem. Br.*, 1975, **11**, 177.

2 R. Hoffman, *Angew. Chem., Int. Ed. Engl.*, 1982, **21**, 711; D. M. P. Mingos, *Acc. Chem. Res.*, 1984, **17**, 311.

3 P. Braunstein and J. Rose, *Comprehensive Organometallic Chemistry*, ed. E. W. Abel, F. G. A. Stone and G. Wilkinson, Pergamon, Oxford, 1995, ch. 7, vol. 10; R. D. Adams, *Polyhedron*, 1988, **7**, 2251; J. Xiao and R. J. Puddephatt, *Coord. Chem. Rev.*, 1995, **143**, 457; M. Cowie, *Can. J. Chem.*, 2005, **83**, 1043; V. Ritleng and M. J. Chetcuti, *Chem. Rev.*, 2007, **107**, 797.

4 L. N. Lewis, *Chem. Rev.*, 1993, **93**, 2693; J. H. Sinfelt, *Bimetallic Catalysts: Discoveries, Concepts, and Applications*, Wiley, New York, 1983; L. D. Menard, Q. Wang, J. H. Kang, A. J. Sealey, G. S. Girolami, X. Teng, A. I. Frenkel and R. G. Nuzzo, *Phys. Rev. B: Condens. Matter*, 2009, **80**, 064111; Y. J. Huang, S. C. Fung, W. E. Gates and G. B. McVicker, *J. Catal.*, 1989, **118**, 192; G. B. McVicker, M. Daage, M. S. Touvelle, C. W. Hudson, D. P. Klein, W. C. Baird, B. R. Cook, J. G. Chen, S. Hantzer and

D. E. W. Vaughan, *J. Catal.*, 2002, **210**, 137; D. W. Flaherty and E. Iglesia, *J. Am. Chem. Soc.*, 2013, **135**, 18586; A. Djeddi, I. Fachete and F. Garin, *Appl. Catal., A*, 2012, **413**, 340; S. G. Ramos, A. Calafiore, A. R. Bonesi, W. E. Triaca, A. M. C. Luna, M. S. Moreno, G. Zampieri and S. Bengio, *Int. J. Hydrogen Energy*, 2012, **37**, 14849; F.-S. Ke, B. C. Solomon, S.-G. Ma and X.-D. Zhou, *Electrochim. Acta*, 2012, **85**, 444; F.-D. Kong, S. Zhang, G.-P. Yin, J. Liu and A.-X. Ling, *Catal. Lett.*, 2014, **144**, 242; S. Hu, L. Xiong, X. Ren, C. Wang and Y. Luo, *Int. J. Hydrogen Energy*, 2009, **34**, 8723.

5 M.-N. Betzile, X. Wang, Z. M. Hudson and S. Wang, *Dalton Trans.*, 2014, **43**, 13696; L. Zhou, C.-L. Kwong, C.-C. Kwok, G. Cheng, H. Zhang and C.-M. Che, *Chem. – Asian J.*, 2014, **9**, 2984; Y. Tanaka, K. M.-C. Wong and V. W.-W. Yam, *Chem. Sci.*, 2012, **3**, 1185; D. R. Striplin and G. A. Crosby, *J. Phys. Chem.*, 1995, **99**, 7977; H.-K. Yip, H.-M. Lin, Y. Wang and C.-M. Che, *Inorg. Chem.*, 1993, **32**, 3402; A. L. Balch and V. J. Catalano, *Inorg. Chem.*, 1992, **31**, 2569; A. Kobayashi and M. Kato, *Eur. J. Inorg. Chem.*, 2014, 4469; A. Diez, E. Lalinde and M. T. Moreno, *Coord. Chem. Rev.*, 2011, **255**, 2426.

6 B. T. Sterenberg, H. A. Jenkins and R. J. Puddephatt, *Organometallics*, 1999, **18**, 219.

7 B. T. Sterenberg, M. C. Jennings and R. J. Puddephatt, *Organometallics*, 1999, **18**, 2162; B. T. Sterenberg, M. C. Jennings and R. J. Puddephatt, *Organometallics*, 1999, **18**, 3737; B. T. Sterenberg, G. J. Spivak, G. P. A. Yap and R. J. Puddephatt, *Organometallics*, 1998, **17**, 2433.

8 R. W. Hilts, O. Oke, M. J. Ferguson, R. McDonald and M. Cowie, *Organometallics*, 2005, **24**, 4393; M. E. Slaney, D. J. Anderson, M. J. Ferguson, R. McDonald and M. Cowie, *Organometallics*, 2012, **31**, 2286; D. S. A. George, R. McDonald and M. Cowie, *Organometallics*, 1998, **17**, 2553.

9 D. M. McEwan, D. P. Markham, P. G. Pringle and B. L. Shaw, *J. Chem. Soc., Dalton Trans.*, 1986, 1809; F. S. M. Hassan, D. P. Markham, P. G. Pringle and B. L. Shaw, *J. Chem. Soc., Dalton Trans.*, 1985, 279; S. W. Carr, P. G. Pringle and B. L. Shaw, *J. Organomet. Chem.*, 1988, **341**, 543.

10 W. A. Schenk and G. H. J. Hilpert, *Chem. Ber.*, 1991, **124**, 433; P. Braunstein, C. D. Debellefon, B. Oswald, M. Ries, M. Lanfranchi and A. Tiripicchio, *Inorg. Chem.*, 1993, **32**, 1638; T. Tanase, R. A. Begum, H. Toda and Y. Yamamoto, *Organometallics*, 2001, **20**, 968.

11 R. D. Adams, B. Captain, M. B. Hall, J. L. Sith Jr. and C. E. Webster, *J. Am. Chem. Soc.*, 2005, **127**, 1007; M. J. Freeman, A. D. Miles, M. Murray, A. G. Orpen and F. G. A. Stone, *Polyhedron*, 1984, **3**, 1093; S. Bhaduri, K. R. Sharma, W. Clegg, G. M. Sheldrick and D. Stalke, *J. Chem. Soc., Dalton Trans.*, 1984, 2851; A. Fumagalli, R. D. Pergola, F. Bonacina, L. Garlaschelli, M. Moret and A. Sironi, *J. Am. Chem. Soc.*, 1989, **111**, 165; D. H. Cao, P. J. Stang and A. M. Arif, *Organometallics*, 1995, **14**, 2733; M. H. Araujo, A. A. Avent, P. B. Hitchcock, J. F. Nixon and M. D. Vargas, *Organometallics*, 1998, **17**, 5460; M. V. Jimenez, E. Sola, A. P. Martinez, F. J. Lahoz and L. A. Oro, *Organometallics*, 1999, **18**, 1125; I. Jourdain, M. Knorr, C. Strohmann, C. Unkelbach, S. Rojo, P. Gomez-Iglesias and F. Villafane, *Organometallics*, 2013, **32**, 5343.

12 M. P. Brown, J. R. Fisher, L. Manojlovic-Muir, K. W. Muir, R. J. Puddephatt, M. A. Thomson and K. R. Seddon, *J. Chem. Soc., Chem. Commun.*, 1979, 931; M. P. Brown, J. R. Fisher, R. H. Hill, R. J. Puddephatt and K. R. Seddon, *Inorg. Chem.*, 1981, **20**, 3516; M. P. Brown, J. R. Fisher, A. J. Mills, R. J. Puddephatt and M. A. Thomson, *Inorg. Chim. Acta*, 1980, **44**, L271; H. C. Foley, R. H. Morris, T. S. Targos and G. L. Geoffroy, *J. Am. Chem. Soc.*, 1981, **103**, 7337; L. Manojlovic-Muir, K. W. Muir, A. A. Frew, S. S. M. Ling, M. A. Thomson and R. J. Puddephatt, *Inorg. Chem.*, 1981, **20**, 1500; R. H. Hill, P. de Mayo and R. J. Puddephatt, *Inorg. Chem.*, 1982, **21**, 3642; J. R. Fisher, A. J. Mills, S. Sumner, M. P. Brown, M. A. Thomson, R. J. Puddephatt, A. A. Frew, Lj. Manojlovic-Muir and K. W. Muir, *Organometallics*, 1982, **1**, 1421; R. H. Hill and R. J. Puddephatt, *J. Am. Chem. Soc.*, 1983, **105**, 5797; A. J. McLennan and R. J. Puddephatt, *Organometallics*, 1986, **5**, 811; M. P. Brown, J. R. Fisher, S. J. Franklin, R. J. Puddephatt and K. R. Seddon, *J. Organomet. Chem.*, 1978, **161**, C46.

13 Z. S. Wilson, G. G. Stanley and D. A. Vicic, *Inorg. Chem.*, 2010, **49**, 5385; W. H. Lam and V. W.-W. Yam, *Inorg. Chem.*, 2010, **49**, 10930; B. J. Burkhart and R. L. DeKock, *Comput. Theor. Chem.*, 2012, **994**, 1.

14 B. Chaudret, B. Delavaux and R. Poilblanc, *Coord. Chem. Rev.*, 1988, **86**, 191; S. M. Oldham, J. F. Houlis, C. J. Leigh, S. B. Duckett and R. Eisenberg, *Organometallics*, 2000, **19**, 2985; R. A. Stockland, G. K. Anderson and N. P. Rath, *J. Am. Chem. Soc.*, 1999, **121**, 7945; B. A. Vaartstra and M. Cowie, *Inorg. Chem.*, 1989, **28**, 3138; B. A. Vaartstra, K. N. O'Brien, R. Eisenberg and M. Cowie, *Inorg. Chem.*, 1988, **27**, 3668; R. McDonald, B. R. Sutherland and M. Cowie, *Inorg. Chem.*, 1987, **26**, 3333; M. C. Grossel, J. R. Batson, R. P. Moulding and K. R. Seddon, *J. Organomet. Chem.*, 1986, **304**, 391; K. A. Azam, A. A. Frew, B. R. Lloyd, L. Manojlovic-Muir, K. W. Muir and R. J. Puddephatt, *Organometallics*, 1985, **4**, 1400; R. J. Puddephatt, K. A. Azam, R. H. Hill, M. P. Brown, C. D. Nelson, R. P. Moulding, K. R. Seddon and M. C. Grossel, *J. Am. Chem. Soc.*, 1983, **105**, 5642.

15 E. A. V. Ebsworth, D. W. H. Rankin, I. M. Blacklaws and H. E. Robertson, *J. Chem. Soc., Dalton Trans.*, 1978, 753; R. J. Puddephatt, *Coord. Chem. Rev.*, 2001, **219**, 157.

16 C. E. Johnson and R. Eisenberg, *J. Am. Chem. Soc.*, 1985, **107**, 6531.

17 P. S. Pregosin and R. W. Kunz, *^{31}P and ^{13}C NMR of Transition Metal Complexes*, Springer-Verlag, Berlin, 1979.

18 W. D. Wang and R. Eisenberg, *Organometallics*, 1992, **11**, 908; M. H. Mobarok, O. Oke, M. J. Ferguson, R. McDonald and M. Cowie, *Inorg. Chem.*, 2010, **49**, 11556.

19 C.-L. Lee, C. T. Hunt and A. L. Balch, *Inorg. Chem.*, 1981, **20**, 2498; R. J. Puddephatt and M. A. Thomson, *Inorg.*

Chem., 1982, **21**, 725; M. Cowie and T. G. Southern, *Inorg. Chem.*, 1982, **21**, 246; K. A. Azam and R. J. Puddephatt, *Organometallics*, 1983, **2**, 1396; J. A. Davies, K. Kirschbaum and C. Kluwe, *Organometallics*, 1994, **13**, 3664; M. J. Irwin, G. Jia, J. J. Vittal and R. J. Puddephatt, *Organometallics*, 1996, **15**, 5321.

20 D. S. A. George, R. McDonald and M. Cowie, *Can. J. Chem.*, 1998, **74**, 2289; D. S. A. George, R. McDonald and M. Cowie, *Organometallics*, 1998, **17**, 2553; H. C. Clark and R. J. Puddephatt, *Inorg. Chem.*, 1971, **10**, 18.

21 A. Albinati, T. J. Emge, T. F. Koetzle, S. V. Meille, A. Musco and L. M. Venanzi, *Inorg. Chem.*, 1986, **25**, 4821.

22 C. P. Kubiak and R. Eisenberg, *J. Am. Chem. Soc.*, 1977, **99**, 6129.

23 C. P. Kubiak, C. Woodcock and R. Eisenberg, *Inorg. Chem.*, 1980, **19**, 2733; M. Cowie and T. G. Southern, *Inorg. Chem.*, 1982, **21**, 246.

24 S. J. Cooper, M. P. Brown and R. J. Puddephatt, *Inorg. Chem.*, 1981, **20**, 1374.

25 C.-M. Che, L. G. Butler and H. B. Gray, *J. Am. Chem. Soc.*, 1981, **103**, 1593; W. A. Fordyce, J. G. Brummer and G. A. Crosby, *J. Am. Chem. Soc.*, 1981, **103**, 7061; D. M. Roundhill, H. B. Gray and C.-M. Che, *Acc. Chem. Res.*, 1989, **22**, 55; M. I. S. Kenney, J. W. Kenney III and G. A. Crosby, *Organometallics*, 1986, **5**, 230; C.-M. Che, V. V.-W. Yam, W.-T. Wong and T.-F. Lai, *Inorg. Chem.*, 1989, **28**, 2908; A. L. Balch and V. J. Catalano, *Inorg. Chem.*, 1992, **31**, 3934; V. W.-W. Yam, P. K.-Y. Yeung, L.-P. Chan, W.-K. Kwok, D. L. Phillips, K.-L. Yu, R. W.-K. Wong, H. Yan and Q.-J. Meng, *Organometallics*, 1998, **17**, 2590; W. H. Lam and V. W.-W. Yam, *Inorg. Chem.*, 2010, **49**, 10930.

26 G. te Velde, F. M. Bickelhaupt, E. J. Baerends, S. van Gisbergen, C. F. Guerra, J. G. Snijders and T. Ziegler, *J. Comput. Chem.*, 2001, **22**, 931; A. Becke, *Phys. Rev. A*, 1988, **38**, 3098.

27 C. Mealli, F. Pichierri, L. Randaccio, E. Zangrando, M. Krumm, D. Holtenrich and B. Lippert, *Inorg. Chem.*, 1995, **34**, 3418; M. P. Brown, S. J. Cooper, A. A. Frew, L. Manojlovic-Muir, K. W. Muir, R. J. Puddephatt, K. R. Seddon and M. A. Thomson, *Inorg. Chem.*, 1981, **20**, 1500; M. Rashidi, M. C. Jennings and R. J. Puddephatt, *Organometallics*, 2003, **22**, 2612; B. Shafaatian, A. Akbari, S. M. Nabavizadeh, F. W. Heinemann and M. Rashidi, *Dalton Trans.*, 2007, 4715.

28 L. Garlaschelli, R. Della Pergola and S. Martinengo, *Inorg. Synth.*, 1990, **28**, 211.

29 (*a*) *Computer programs (a) COLLECT, DENZO, SCALEPACK*, Nonius B. V., Amsterdam, 1998; (*b*) G. M. Sheldrick, *SHELXTL*, Madison, Wisconsin, Release 97-2, 1998, Release 2014-1, 2014; (*c*) L. J. Farrugia, *J. Appl. Crystallogr.*, 1999, **32**, 837.